*Protein Science* (1995), *4*:1490–1497. Cambridge University Press. Printed in the USA.


# Formation of ion channels in lipid bilayers by a peptide with the predicted transmembrane sequence of botulinum neurotoxin A

MYRTA OBLATT-MONTAL, MASAHITO YAMAZAKI, RICHARD NELSON, AND MAURICIO MONTAL

Department of Biology, University of California San Diego, La Jolla, California 92093-0366

(RECEIVED February 23, 1995; ACCEPTED May 25, 1995)

**Abstract**

Synthetic peptides patterned after the predicted transmembrane sequence of botulinum toxin A were used as tools to identify an ion channel-forming motif. A peptide denoted BoTxATM, with the sequence GAVILLEFIPEIAI PVLGTFALV, forms cation-selective channels when reconstituted in planar lipid bilayers. As predicted, the self-assembled conductive oligomers express heterogeneous single-channel conductances. The most frequent openings exhibit single-channel conductance of 12 and 7 pS in 0.5 M NaCl, and 29 and 9 pS in 0.5 M KCl. In contrast, ion channels are not formed by a peptide of the same amino acid composition as BoTxATM with a scrambled sequence. Conformational energy calculations show that a bundle of four amphipathic α-helices is a plausible structural motif underlying the measured pore properties. These studies suggest that the identified module may play a functional role in the ion channel-forming activity of intact botulinum toxin A.

**Keywords:** botulinum toxin; ionic channels; lipid bilayers; neurotransmitter release; protein design; synaptic vesicle fusion; tetanus toxin

Botulinum neurotoxins, a family of bacterial proteins secreted by *Clostridium botulinum*, are potent blockers of synaptic transmission in peripheral cholinergic nervous system synapses, thereby causing paralysis (Simpson, 1989; Montecucco & Schiavo, 1994). Recent studies on the biochemical dissection of the components involved in the fusion of secretory vesicles with the plasma membrane have set BoTxs at the center of this process. The current excitement arises from the finding that BoTxs are $Zn^{2+}$-metalloproteases that selectively cleave proteins implicated in the fusion process and, accordingly, block neurotransmitter release into the synaptic cleft (cf. Bennett & Scheller, 1994; Ferro-Novick & Jahn, 1994; Jahn & Sudhof, 1994; Rothman, 1994; Schiavo et al., 1994; Sollner & Rothman, 1994). Notably, BoTx isoforms A, E, and C cleave the plasma membrane-associated proteins SNAP-25 (synaptosome-associated protein of 25 kDa) (BoTxA and BoTxE) and syntaxin (BoTxC) (Blasi et al., 1993a, 1993b; Schiavo et al., 1993a, 1993b; Binz et al., 1994), whereas BoTxB, D, F, and G proteolyze synaptobrevin, a vesicle-associated membrane protein, also known as VAMP (Schiavo et al., 1992a, 1992b, 1993a, 1993b; Hayashi et al., 1994; Yamasaki et al., 1994).

The protease activity of the toxins is confined to their light chain, $M_r$ 50 kDa, which is disulfide linked to a heavy chain, $M_r$ 100 kDa, necessary for toxin internalization (Montecucco et al., 1994). BoTxs have an inherent propensity to insert into membranes, especially at acidic pH (cf. Montecucco et al., 1991; Schiavo et al., 1994). This property is compatible with the ion-channel activity observed when BoTxA, B, C, D, and E are reconstituted in lipid bilayers (Hoch et al., 1985; Donovan & Middlebrook, 1986; Blaustein et al., 1987). It has been proposed that such a channel is the conduit through which the LC gets access to the cytosol, where it acts (Boquet et al., 1976; Hoch et al., 1985; Donovan & Middlebrook, 1986; Blaustein et al., 1987).

The amino-terminal domain of the HC appears involved in membrane insertion and translocation (for review see Montecucco et al., 1994) and contains the channel-forming activity of BoTxA (Blaustein et al., 1987) (see Kinemages 1 and 2). Sequence analysis suggests the occurrence in this domain of an amphipathic stretch sufficiently long to span the width of the bilayer as a transmembrane helix (Montal et al., 1992; Lebeda

Reprint requests to: Mauricio Montal, Department of Biology, University of California San Diego, La Jolla, California 92093-0366; e-mail: montal@jeeves.ucsd.edu.

*Abbreviations:* BoTxs, botulinum neurotoxins; BoTxA, botulinum neurotoxin serotype A; TeTx, tetanus toxin; HC, heavy chain; LC, light chain; $\gamma$, single-channel conductance; TM, transmembrane segment; POPE, 1-palmitoyl-2-oleyl-*sn*-glycero-3-phosphoethanolamine; POPC, 1-palmitoyl-2-oleyl-*sn*-glycero-3-phosphocholine; $\tau_c$, closed time; $\tau_o$, open time.

et al., 1994). Conformational energy calculations suggest that such a motif is thermodynamically feasible and compatible with the assembly of a transmembrane channel by the clustering of four α-helices (Montal et al., 1992). Image reconstruction analysis of electron micrographs of BoTx inserted in membranes suggests the occurrence of a tetramer as the structural entity underlying the BoTx channel (Schmid et al., 1993).

Here we report that a peptide with a sequence corresponding to the amphipathic segment of BoTxA HC forms ion channels in lipid bilayers, supporting the notion that the HC may act as a channel through which the LC enters the cytosol. A similar motif for the structurally homologous tetanus toxin has been described (Montal et al., 1992), which, in concert with the findings reported here, lends support to the model.

## Results and discussion

### *Sequence analysis*

Amino acid sequence analysis suggests the occurrence of a potential transmembrane segment in BoTxA HC. This segment encompasses amino acids 659–681, with sequence GAVILLE FIPEIAIPVLGTFALV. Hydropathic power spectral analysis (Eisenberg et al., 1984; Greenblatt et al., 1985) confirms the assignment and predicts an amphipathic α-helical structure (Montal et al., 1992). A peptide with a sequence corresponding to this segment, denoted as BoTxATM, was synthesized and purified by HPLC. Electrospray mass analysis (Schnolzer et al., 1992) of the HPLC peak (Fig. 1) shows three peaks for the +3 ($m/z$ = 799.5), +2 ($m/z$ = 1,198.5), and +1 ($m/z$ = 2,396.0) charged states. This profile corresponds to a peptide with a measured mass of 2,395.2 ± 0.3 Da, the expected molecular mass (calculated monoisotopic and average isotope compositions of 2,394.4 and 2,395.96 Da, respectively), in accord with the anticipated amino acid composition of the peptide. Mass analysis, therefore, indicates that the molecule is the target BoTxATM peptide of high purity.

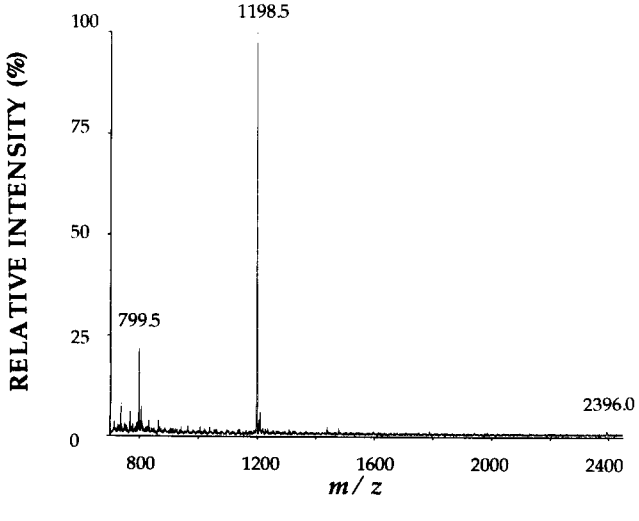


**Fig. 1.** Mass spectrum of the purified BoTxATM synthetic peptide. $m/z$ is the mass-to-charge ratio. Numbers are the mass of the indicated species.

### *Channel formation by BoTxATM*

BoTxATM peptide forms ionic channels after reconstitution in lipid bilayers; this is shown in Figure 2. A 12-second segment from a continuous recording that lasted several minutes is displayed in Figure 2A. Well-defined levels of current reflect the occurrence in the membrane of several discrete conductive entities of distinct single-channel conductances. Sections of the record indicated by the letters B, C, and D are displayed at higher time resolution in Figure 2B, C, and D, respectively. Figure 2E displays a section of the record starting 66 s from the beginning. The amplitude of the most frequent openings are of 10 pS, 29 pS, and combinations of these two values that give rise to transitions, with apparent $\gamma \approx 20$ pS and 40 pS. Thus, the conductance events are heterogeneous in amplitude.

Bursts of channel activity in which the predominant species dominate the window of recording are used to assess the nature of the underlying process. The most frequent events have $\gamma$ = 12 ± 1 pS and 6.5 ± 1 pS ($n$, number of experiments, = 17) in symmetric 0.5 M NaCl (Fig. 3A,B), and 29 ± 2 pS and 9 ± 1 pS ($n$ = 37) in 0.5 M KCl (Fig. 3C,D). The current histograms identify the occurrence of two discrete states, closed and open, for these primary conductances; these are illustrated in Fig-

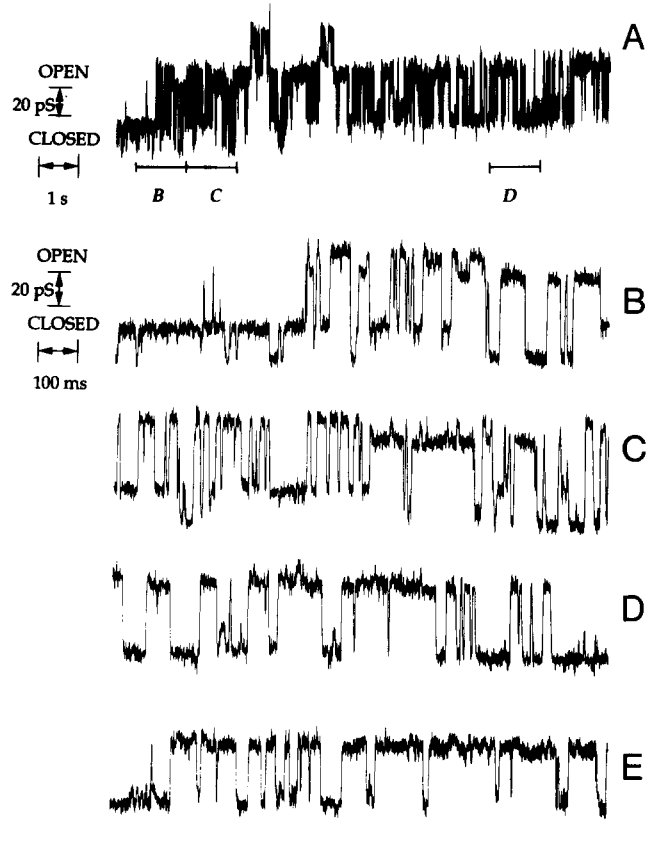


**Fig. 2.** BoTxATM peptide forms ion channels in lipid bilayers. Lipid bilayers were composed of POPE/POPC and studied in symmetric 0.5 M KCl, 1 mM $CaCl_2$, 5 mM Hepes, pH 7.4. Currents were recorded at $V$ = 100 mV. Upward deflections indicate channel openings. **A:** A 12-s segment of a continuous recording displayed at low time resolution. **B,C,D,E:** Recordings displayed at a higher time resolution (note different time scale calibrations). Records filtered at 1 kHz.

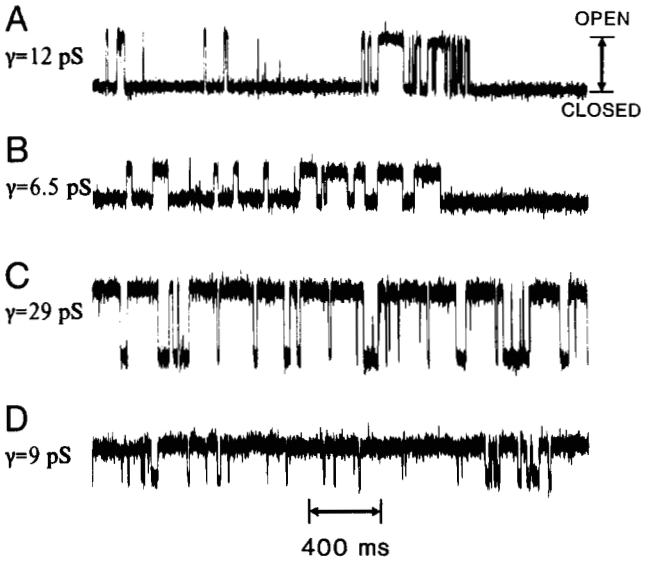


**Fig. 3.** Single-channel currents from POPE/POPC bilayers containing the BoTxATM peptide. Currents were recorded at $V = 100$ mV in symmetric 0.5 M NaCl (A,B) or KCl (C,D), 1 mM $CaCl_2$, 5 mM Hepes, pH 7.4. Segments of a continuous record are displayed to illustrate the occurrence of the **(A)** 12-pS channel; **(B)** 6.5-pS channel in NaCl; and **(C)** 29-pS channel and **(D)** 9-pS channel in KCl. Records filtered at 2 kHz.

ure 4A for the $\gamma = 29$-pS channel in KCl and Figure 4B for the $\gamma = 12$-pS channel in NaCl. The primary conductances are ohmic as determined from current-voltage ($I$-$V$) relationships. Discrete openings with smaller or larger conductances are also discerned: In NaCl, distinct openings with $\gamma = 21 \pm 2$ pS are interspersed among the primary conductances, whereas in KCl, such openings display conductances of $20 \pm 2$ pS and $42 \pm 2$ pS. Their occurrence is sporadic and the channel open times of the larger conductance events are significantly shorter than those of the primary conductances. The heterogeneity of conductance species observed with BoTxATM, both in amplitude and in the time that the channels remain open, is anticipated for an amphipathic peptide that self-assembles in the membrane to form noncovalent conductive oligomers of different sizes (Oiki et al., 1988, 1990; Montal et al., 1990; cf. Montal, 1995).

The most common pattern of channel occurrences is in the form of bursts of activity. Within these bursts of activity, the residence times of the channels in the open or closed states are not uniform, yet they present a consistent pattern with occurrences that are very short-lived (<1 ms) and others that have residence times of several hundred milliseconds. In general, both the open channel lifetimes and the closed times are best fitted by the sum of two exponentials. For example, in KCl for the openings with $\gamma = 29$ pS, the $\tau_{o1} = 0.8 \pm 0.1$ ms and $\tau_{o2} = 49 \pm 5$ ms for the open times and $\tau_{c1} = 0.7 \pm 0.2$ ms and $\tau_{c2} = 42 \pm 5$ ms for the closed times ($n = 3$). In NaCl, the residence time of the channels in the open state appears shorter than in KCl. This is reflected in the conductance histograms (Fig. 4A,B) in which the area under the curve corresponding to the open state is larger for KCl than for NaCl. This result is representative for the other conductance species and tends to produce recordings in KCl that appear more active than in NaCl. These findings may arise from different structure and stability of the conductive oligomers in $Na^+$ or $K^+$.

### *pH dependence of channel formation by BoTxATM*

The activity of BoTxATM peptide was studied at pH 4.8. This condition, which mimics the pH prevalent inside endosomes, is considered critical for the intracellular processing and routing of the toxin. The results are undecisive. This stems from the fact that the peptide is practically insoluble at pH 4.8. Reconstitution from the aqueous phase results in precipitation of the peptide. Incorporation from the lipid phase has produced unreliable results. The data imply that the conformational change undergone by the holotoxin at acidic pH (Boquet et al., 1984; cf. Montecucco & Schiavo, 1994) may be required to expose the transmembrane sequence for eventual incorporation into the endosomal membrane. For the isolated segment, however, the

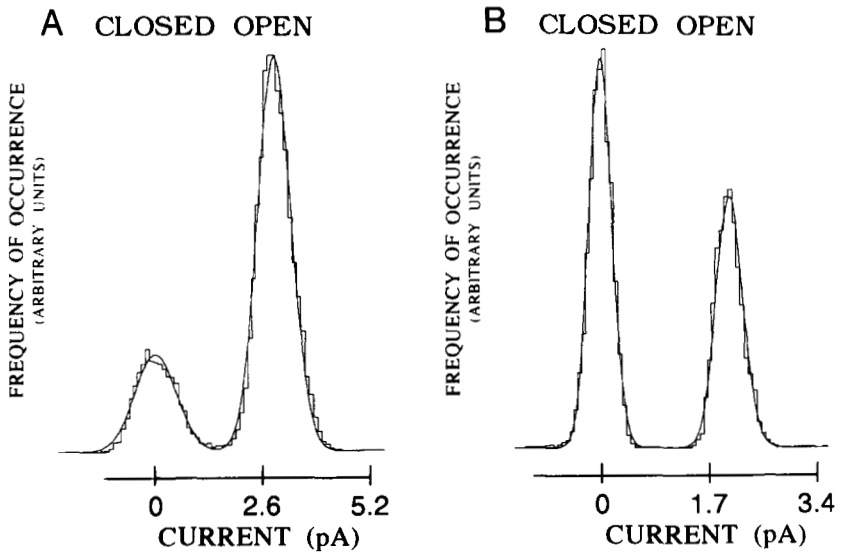


**Fig. 4.** Current histograms for the primary conductances, generated from continuous segments of records lasting several minutes, are displayed **(A)** for KCl and **(B)** for NaCl; CLOSED and OPEN denote closed and open states. The probability of the channel being open, $P_o$, or closed, $P_c$, is calculated from the area under the corresponding Gaussian curve (Labarca et al., 1985; Montal et al., 1986; Gambale & Montal, 1988; Grove et al., 1992). In NaCl, $P_o = 0.43$; in KCl, $P_o = 0.77$. The single-channel current is calculated as the difference between the peaks associated with the closed and open states. Currents were recorded at $V = 100$ mV (A) and $V = 200$ mV (B). The corresponding values for single-channel conductances are 29 pS (KCl) and 12 pS (NaCl). Records filtered at 1 kHz.

exposure step is not required and may in fact determine its precipitation in the aqueous phase rather than its insertion into the bilayer.

### *Sequence specificity*

A peptide of the same amino acid composition as BoTxATM but with a computer-generated random sequence, predicted to retain a propensity for $\alpha$-helix formation, was synthesized. The sequence is EAVLLILIFPALGIPIGVTAFVE. This peptide interacts with bilayers, as manifested by stray fluctuations in membrane current. However, the peptide with the randomized sequence differs from BoTxATM in that it does not form discrete conducting events ($n = 4$ experiments). These results support the specificity of the identified sequence as a candidate for the pore.

### *Comparison of the channel properties of the BoTxATM peptide and of the TeTx peptide, a peptide with the predicted transmembrane sequence of tetanus toxin*

Previous work led to the identification of a similar transmembrane motif in the primary structure of tetanus toxin (Montal et al., 1992). A peptide with such sequence, denoted as TeTx in Figure 5A, forms channels in lipid bilayers. The most frequent openings have $\gamma = 28 \pm 3$ pS in 0.5 M NaCl and $\gamma = 24 \pm 2$ pS in 0.5 M KCl. By way of comparison, the conductance of the BoTxATM channel is significantly lower in NaCl, $\gamma = 12 \pm 1$ pS, yet similar in KCl, $\gamma = 29 \pm 2$ pS. The residence times of the channels in the open state are shorter for the BoTxATM channel than for the TeTx channel. These disparities may reflect specific differences in the pore-lining residues or distinct oligomeric structures of the conductive species.

### *Inferences about a functional role of this protein module and its putative structure*

All isoforms of BoTx form ion channels in lipid bilayers (Hoch et al., 1985; Donovan & Middlebrook 1986; Blaustein et al., 1987; cf. Finkelstein, 1990). TeTx forms cation-selective channels in lipid bilayers (Borochov-Neori et al., 1984; Hoch et al., 1985; Gambale & Montal, 1988; Rauch et al., 1990; cf. Finkelstein, 1990) and in neural cells (Beise et al., 1994). For all these toxins, channel formation is more effective at acidic pH.

The amino-terminal fragments of the heavy chains of the neurotoxins form channels that, at pH 7.0, exhibit heterogeneous conductances. For BoTxB, the most frequent openings exhibit $\gamma = 15$ pS, whereas for TeTx $\gamma = 45$ pS, in 1 M KCl (Hoch et al., 1985). At pH 4.0, the predominant single-channel conductances were $\gamma = 20$ pS and $\gamma = 15$ pS, respectively (Hoch et al., 1985). These latter values approximate those measured at neutral pH with the peptide mimics BoTxATM and TeTx. This suggests that pH may be necessary to drive a conformational change in the holotoxin, thereby exposing the transmembrane sequence, which then inserts into the bilayer core and eventually assembles into a conductive oligomer.

The finding that all these toxins that act intracellularly enter cells by endocytosis has suggested that the acid pH of endocytic vesicles induces a conformational change that promotes insertion of the HC of the toxins into and across the endosomes, therefore allowing the translocation of the LC catalytic moiety into the cytosol, where it acts (Boquet et al., 1976, 1984; Boquet & Duflot, 1982; Borochov-Neori et al., 1984; Hoch et al., 1985; Donovan & Middlebrook, 1986; Blaustein et al., 1987; Gambale & Montal, 1988; cf. Simpson, 1989, Finkelstein, 1990; Rauch et al., 1990; Montecucco et al., 1991, 1994). This model implies that toxin translocation and channel formation are related phenomena (see also Schmid et al., 1994).

A

```
                *   * *  **   *
BoTxA       GAVILLEFIPEIAIPVLGTFALV
BoTxB       GASILLEFIPELLIPVVGAFLLE
BoTxC       GVTILLEAFPEFTIPALGAFVIY
BoTxD       GVAFLLEGFPEFTIPALGVFTFY
BoTxE       GAGILLEFEPELLIPTILVFTIK
BoTxF       GVGILLEFVPELTIPVILVFTIK
BoTxG       GAAILMEFIPELIVPIVGFFTLE
TeTX        GVVLLLEYIPEITLPVIAALSIA
Consensus   GAAILLEFIPELTIPVIGAFTIE
```

B

```
               **   * *** *  * ***
BoTxA       DPAVTLAHELIHAGHRLYG
BoTxB       DPALILMHELIHVLHGLYG
BoTxC       DPILILMHELNHAMHNLYG
BoTxD       DPVIALMHELTHSLHQLYG
BoTxE       DPALTLMHELIHSLHGLYG
BoTxF       DPAISLAHELIHALHGLYG
BoTxG       DPALTLMHELIHVLHGLYG
TeTX        DPALLLMHELIHVLHGLYG
Consensus   DPALTLMHELIHALHGLYG
```

**Fig. 5. A:** Alignment of the predicted transmembrane sequence in the heavy chain of the seven isoforms of BoTx, of TeTx, and the calculated consensus sequence. **B:** Alignment of the zinc-binding motif in the light chain of the seven isoforms of BoTx, of TeTx, and the calculated consensus sequence. Identical residues are indicated by the asterisk. For BoTxA, the segments illustrated correspond to amino acids 659–681 (A) and 215–233 (B) of the actual protein sequence.

The toxin HC segment represented by the BoTxATM peptide is highly conserved in all BoTx isoforms and in TeTx, as indicated by the alignment shown in Figure 5A. The consensus sequence suggests a functional role for this conserved motif. BoTxATM is amphipathic and, when inserted in a membrane, presumably assembles into an oligomeric transmembrane structure. The tetrameric organization inferred from image reconstruction analysis (Schmid et al., 1993) suggests that a channel structure may be modeled as a four-helix bundle. Conformational energy calculations indicate that a four-helix bundle structure conserved in all BoTxs and in TeTx may be compatible with the channels observed after reconstitution of intact toxins or their fragments in bilayers. A stereo view of an energy-minimized structure of a homomeric four-helix bundle of BoTxATM is displayed in Figure 6A and Kinemage 1. The exterior of the bundle exposes primarily hydrophobic residues that presumably interact with the bilayer interior. The bundle lines a hydrophilic pore as depicted by the corresponding dotted contour shown in Figure 6B. The helices are tilted with interhelical angles in the range of 16–22°, consistent with values described for transmembrane $\alpha$-helices in the crystal structure of the photosynthetic reaction center (Deisenhofer & Michel, 1991) and in the helical

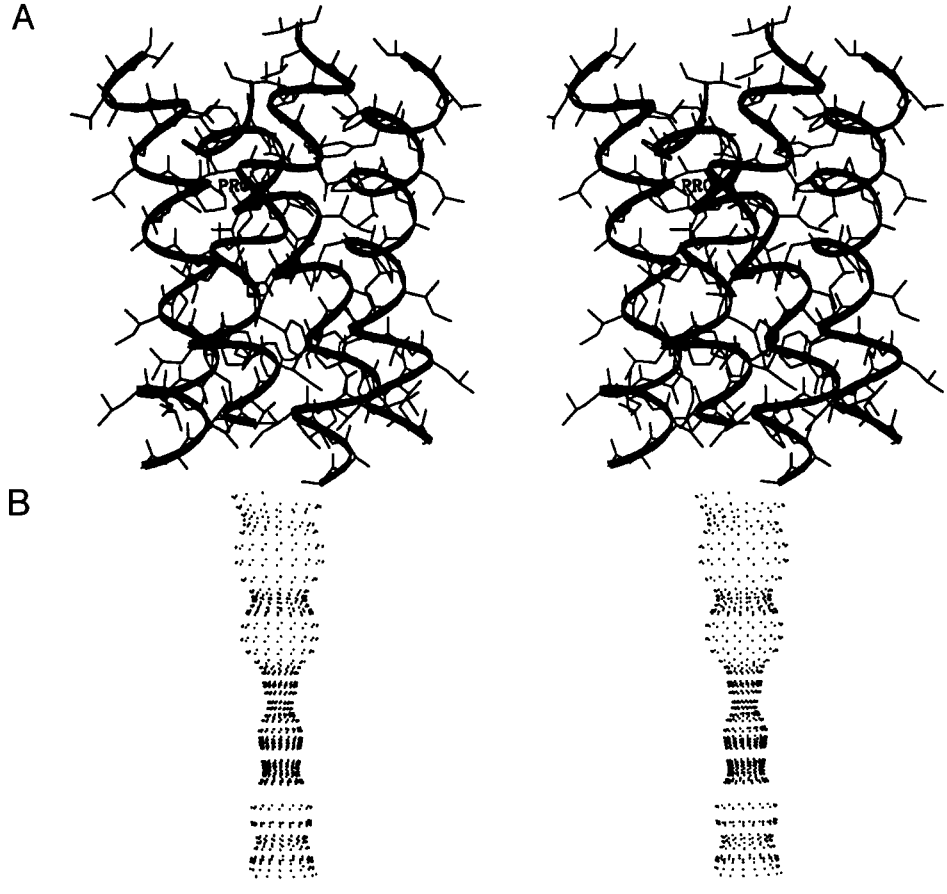


**Fig. 6.** Computer-generated molecular model of the ion channel motif formed by BoTxATM. Stereo views of the energy optimized bundle consisting of four α-helices with the sequence of the BoTxATM. The model represents the BoTxATM segment in a parallel tetrameric arrangement with $C_4$ symmetry. **A:** Side view with the C-terminus on top. The α-carbon backbone is represented with ribbons. PRO, indicates the location of proline 15 (Fig. 5A). **B:** Dotted contours showing the profile of the ion-conductive pathway generated by the four-helix bundle. The two major constrictions in the pore pathway are generated by rings of E11 carboxylates (the narrowest), and the aromatic rings of F8. The distance between opposing carboxylates at position 11 is 1.8 Å.

bundles of cholera toxin and enterotoxin (Sixma et al., 1993a, 1993b; Merritt et al., 1994). The helices bend at their midpoint, concordant with the occurrence of conserved prolines at positions 10 and 15, thereby widening the pore. Transverse sections across the bundle (not shown) indicate the occurrence of two rings of carboxylates (positions 7 and 11) and a square vestibule formed by the aromatic rings of F8, features that may explain the cation selectivity of the toxin channel. These two glutamates are identical in all isoforms of BoTx and in TeTx (Fig. 5). The charged glutamates were stabilized by the presence of two $K^+$ ions inside the pore during the simulation. The narrowest region of the pore occurs at position E11, yielding an apparent pore diameter of 1.8 Å (Fig. 6B). Without the $K^+$ ions, the glutamates repel each other to a distance of 3.7 Å (data not shown). The pore diameter at E7 is 4.0 Å; however, access to the pore was partially hindered by F8. The aromatic ring of F8 formed a cage around a $K^+$ ion during the simulations, yielding an apparent pore diameter of 2.6 Å. It has been suggested that a cage of $\pi$ orbital electrons may contribute to the $K^+$ selectivity of potassium channels (Kumpf & Dougherty, 1993). The hydrophilic residue T19 also faces the pore lumen and may participate in determining aspects of permeation. The hydroxyl group of T19 produces a discrete narrowing near the C-terminal boundary of the bundle; the pore diameter is 5.1 Å. Two hydrophobic residues, V3 and P15, also face the pore lumen with apparent pore diameters of 3.7 Å and 4.0 Å. Hence, bundles of amphipathic α-helices fit the structural and energetic requirements to form the cation-selective pore identified in reconstitution studies of the intact toxins in lipid bilayers (Oiki et al., 1990; Montal et al., 1992). What the structure of the pore motif will be in the context of the intact protein remains to be seen.

The helical bundle motif is reminiscent of that determined in the crystal structures of three water-soluble bacterial toxins (see Kinemage 2), i.e., the B subunit pentamers of *Escherichia coli* heat-labile enterotoxin (Sixma et al., 1993a, 1993b), verotoxin-1 (Stein et al., 1992), and cholera toxin (Merritt et al., 1994). These helical bundles are pentameric and, in this respect, are similar to the inner bundle that lines the pore of the nicotinic acetylcholine receptor from *Torpedo* electric organs, as determined with cryoelectronmicroscopy to 9 Å resolution (Unwin, 1993, 1995). A heptahelical bundle motif with a central channel has been proposed as the structure that allows access of substrate peptides

into the proteolytic cavity of the 20S proteasome, a key ATP-dependent protease involved in the ubiquitin pathway of protein degradation (Lupas et al., 1994).

The toxin channel is conjectured to be involved in the translocation of the protein across the endocytic vesicle that exposes the LC protease to the cytosol. The dimensions of the channel, inferred from lipid bilayer measurements of single-channel conductance and cut-off size of permeant ions, suggest that a pore diameter of ~8 Å would be compatible with the permeation pathway required for an extended peptide chain (Hoch et al., 1985; Blaustein et al., 1987; Finkelstein, 1990). It is noteworthy that the enterotoxin structure shows that its channel contains an extended peptide, lending support to the notion that a helical bundle motif is compatible with a presumptive peptide channel structure (Sixma et al., 1993a). Further, protein-conducting channels from endoplasmic reticulum (Simon & Blobel, 1991), *E. coli* bacterial membranes (Simon & Blobel, 1992), and mitochondrial outer membrane (Mayer et al., 1995) have been reported.

The crystal structure of BoTxA is not yet available (Stevens et al., 1991). Notwithstanding, two functional modules have been uncovered in the protein sequence: one in the LC; the other in the HC (Fig. 5A,B). Biochemical and electrophysiological studies led to the identification of a $Zn^{2+}$-binding motif in BoTx and TeTx LCs (Fig. 5B), and to the discovery that these neurotoxins are zinc-proteases (cf. Hooper, 1994; Montecucco & Schiavo, 1994; Schiavo et al., 1994). Our findings suggest that the identified module in the neurotoxin's HC (Fig. 5A) may play a functional role in the ion channel-forming activity of the intact botulinal and tetanus toxins. Identification of this functional module and the single-channel assay of its activity may provide opportunities for screening and designing BoTxA channel blockers directed to abrogate the translocation of the BoTxA LC into the cytosol and, presumably, interfere with its cellular toxicity.

## Materials and methods

### *Peptide synthesis, purification, and reconstitution in lipid bilayers*

Peptides were synthesized by Boc-chemistry solid-phase methods on polystyrene resins using an Applied Biosystems model 431 peptide synthesizer (ABI, Foster City, California) (cf. Grove et al., 1992). Peptides were purified by reversed-phase HPLC on an Applied Biosystems HPLC system. Vydac columns, C4 analytical (5 μm, 4.6 × 250 mm) and C4 semipreparative (10 μm, 10 × 250 mm), were used. Typical analytical runs used a linear gradient (20–80 %B) over 60 min at a constant flow rate of 1 mL/min; buffer A was 0.1% trifluoroacetic acid in water and buffer B was 0.1% trifluoroacetic acid in 90% acetonitrile/10% water (v/v). The purified peptides were analyzed by electrospray ionization mass spectrometry using a triple quadrupole mass spectrometer (model API III, Sciex, Thornhill, Ontario, Canada); ionization was conducted at a flow rate of 4 μL/min, as described (Schnolzer et al., 1992). Lipid bilayers were formed at the tip of patch pipets by apposition of two monolayers (Montal & Mueller, 1972; Suarez-Isla et al., 1983; Montal et al., 1986; Grove et al., 1992; Oblatt-Montal et al., 1993). Lipid monolayers were spread from a lipid solution in hexane (5 mg/mL); the lipids used were 4:1 POPE/POPC (Avanti Biochemicals, Alabaster, Alabama). Peptides were dissolved in trifluoroethanol and added to the aqueous subphase after bilayer formation. The aqueous subphase was composed of 0.5 M KCl or NaCl, 1 mM $CaCl_2$, and 5 mM Hepes, pH 7.4, unless otherwise indicated. Bilayer experiments were performed at 24 ± 2 °C. Acquisition and analysis of single-channel currents were as described (Labarca et al., 1985; Montal et al., 1986; Gambale & Montal, 1988; Grove et al., 1992). Records were filtered with an 8-pole Bessel filter (Frequency Services, Haverhill, Massachusetts) and digitized at 0.5-ms sampling interval using an Axon TL-1 interface (Axon Instruments, Burlingame, California) connected to an Everex Step 386 computer (Everex, Fremont, California). pClamp 5.5 package (Axon Instruments) was used for data processing. The channel recordings illustrated are representative of the most frequently observed conductances under the specified experimental conditions. Single-channel conductance, $\gamma$, was calculated from Gaussian fits to currents histograms, and channel open ($\tau_o$) and closed ($\tau_c$) lifetimes were calculated from exponential fits to probability density functions (Labarca et al., 1985; Montal et al., 1986). Openings with $\tau_o \leq 0.3$ ms were ignored. $n$ denotes number of experiments and $N$, number of events. $\gamma$, $\tau_o$, and $\tau_c$ were calculated from segments of continuous recordings lasting $t > 45$ s and with $N \geq 500$ events; data from different experiments are reported as mean ± SEM. The data reported include statistical analysis of >7,000 single-channel openings.

### Sequence analysis

Protein sequences were obtained from the GenBank database. Alignments were determined with the progressive alignment algorithm, using the PAM 250 mutation matrix with a gap opening penalty of 8, according to Feng and Doolittle (1990). These programs were ported to run on a Silicon Graphics IRIS 4D/210 GTXB workstation and modified to take advantage of the expanded resources of the workstation. The alignment program was modified to generate the consensus sequence, defined as the most frequent residue at a given position.

### *Conformational energy computations*

Molecular modeling, energy minimization, and molecular dynamics simulations, were conducted on a Silicon Graphics IRIS 4D/210 GTXB workstation using the INSIGHT and DISCOVER molecular modeling packages of Biosym (San Diego, California) (Oiki et al., 1990; Montal et al., 1990, 1992). Low-energy arrangements of α-helices and four-helix bundles were calculated with semiempirical potential energy functions and optimization routines. The model was refined with a four-step protocol: energy minimization, 50-ps molecular dynamics, calculation of the time-averaged structure, and reminimization. The initial structure displayed parallel helices. No constraints were used to force or prevent the helices from tilting during the energy refinement calculations. Hydrogen bonds in α-helices were constrained during the minimization. Constraints were used for symmetry and to maintain regular helical backbone dihedral angles of $\phi = -45°$ and $\psi = -60°$ (Oiki et al., 1990). Two $K^+$ ions were included inside the pore at the level of F8 and E11. The ions were fixed and the system was refined again by energy minimization. A dielectric constant of 4.0 was used for the external environment in the dynamics simulations. Pore contours

and diameters were calculated using the HOLE program, kindly provided by Dr. O. Smart (Smart et al., 1993).

## Acknowledgments

We thank Stephen B.H. Kent (The Scripps Research Institute) for the use of his mass spectrometry facility and for valuable comments, Oliver Smart (Birkbeck College, University of London) for providing the HOLE program, and A.V. Ferrer-Montiel and the anonymous referees of the manuscript for valuable comments. This work was supported by grants from the Department of the Army Medical Research (DAMD 17-93-C-3100) and the Human Frontier Science Program. R.N. is a Predoctoral Trainee (NIH-5T32GM08326).

## References

Beise J, Hahnen J, Andersen-Beckh B, Dreyer F. 1994. Pore formation by tetanus toxin, its chain and its fragments in neuronal membranes and evaluation of the underlying motifs in the structure of the toxin molecule. *Naunyn-Schmiedeberg's Arch Pharmacol 349*:66-73.

Bennett M, Scheller RH. 1994. A molecular description of synaptic vesicle membrane trafficking. *Annu Rev Biochem 63*:63-100.

Binz T, Blasi J, Yamasaki S, Baumeister A, Link E, Sudhof TC, Jahn R, Niemann H. 1994. Proteolysis of SNAP-25 by types E and A botulinal neurotoxins. *J Biol Chem 269*:1617-1620.

Blasi J, Chapman ER, Link E, Binz T, Yamasaki S, DeCamilli P, Sudhof TC, Niemann H, Jahn R. 1993a. Botulinum neurotoxin A selectively cleaves the synaptic protein SNAP-25. *Nature 365*:160-163.

Blasi J, Chapman ER, Yamasaki S, Binz T, Niemann H, Jahn R. 1993b. Botulinum neurotoxin C1 blocks neurotransmitter release by means of cleaving HPC-1/syntaxin. *EMBO J 12*:4821-4828.

Blaustein RO, Germann WJ, Finkelstein A, DasGupta BR. 1987. The N-terminal half of the heavy chain of botulinum type A neurotoxin forms channels in planar phospholipid bilayers. *FEBS Lett 226*:115-120.

Boquet P, Duflot E. 1982. Tetanus toxin fragment forms channels in lipid vesicles at low pH. *Proc Natl Acad Sci USA 79*:7614-7618.

Boquet P, Duflot E, Hauttecoeur B. 1984. Low pH induces a hydrophobic domain in the tetanus toxin molecule. *Eur J Biochem 144*:339-344.

Boquet P, Silverman MS, Pappenheimer AM Jr, Vernon WB. 1976. Binding of triton-X 100 to diphtheria toxin, crossreacting material 45, and their fragments. *Proc Natl Acad Sci USA 73*:4449-4453.

Borochov-Neori H, Yavin E, Montal M. 1984. Tetanus toxin forms channels in lipid bilayers containing gangliosides. *Biophys J 45*:83-85.

Deisenhofer J, Michel H. 1991. High-resolution structures of photosynthetic reaction centers. *Annu Rev Biophys Biophys Chem 20*:247-266.

Donovan JJ, Middlebrook JL. 1986. Ion-conducting channels produced by botulinum toxin in planar lipid membranes. *Biochemistry 25*:2872-2876.

Eisenberg D, Schwarz E, Komaromy M, Wall R. 1984. Analysis of membrane and surface protein sequences with the hydrophobic moment plot. *J Mol Biol 179*:125-142.

Feng DF, Doolittle RF. 1990. Progressive alignment and phylogenetic tree construction of protein sequences. *Methods Enzymol 183*:375-387.

Ferro-Novick S, Jahn R. 1994. Vesicle fusion from yeast to man. *Nature 370*:191-193.

Finkelstein A. 1990. Channels formed in phospholipid bilayer membranes by diphtheria, tetanus, botulinum and anthrax toxin. *J Physiol 84*: 188-190.

Gambale F, Montal M. 1988. Characterization of the channel properties of tetanus toxin in planar lipid bilayers. *Biophys J 53*:771-783.

Greenblatt RE, Blatt Y, Montal M. 1985. The structure of the voltage-sensitive sodium channel: Inferences derived from computer-aided analysis of the *Electrophorus electricus* channel primary structure. *FEBS Lett 193*:125-134.

Grove A, Iwamoto T, Montal MS, Tomich JM, Montal M. 1992. Synthetic peptides and proteins as models for pore-forming structure of channel proteins. *Methods Enzymol 207*:510-525.

Hayashi T, McMahon H, Yamasaki S, Binz T, Hata Y, Sudhof TC, Niemann H. 1994. Synaptic vesicle membrane fusion complex: Action of clostridial neurotoxins on assembly. *EMBO J 13*:5051-5061.

Hoch DH, Romero-Mira M, Erlich B, Finkelstein A, DasGupta BR, Simpson LL. 1985. Channels formed by botulinum, tetanus, and diphteria toxins in planar lipid bilayers: Relevance to translocation of proteins across membranes. *Proc Natl Acad Sci USA 82*:1692-1696.

Hooper NM. 1994. Families of zinc metalloproteases. *FEBS Lett 354*:1-6.

Jahn R, Sudhof TC. 1994. Synaptic vesicles and exocytosis. *Annu Rev Neurosci 17*:219-246.

Kumpf RA, Dougherty DA. 1993. A mechanism for ion selectivity in potassium channels: Computational studies of cation-pi interactions. *Science 261*:1708-1710.

Labarca P, Rice J, Fredkin D, Montal M. 1985. Kinetic analysis of channel gating. Application to the cholinergic receptor channel and the chloride channel from *Torpedo californica*. *Biophys J 47*:469-478.

Lebeda FJ, Hack DC, Gentry MK. 1994. Theoretical analyses of the functional regions of the heavy chain of botulinum neurotoxin. In: Jankovic J, Hallett M, eds. *Therapy with botulinum toxin*. New York: Marcel Dekker. pp 51-61.

Lupas A, Koster AJ, Walz J, Baumeister W. 1994. Predicted secondary structure of the 20 S proteasome and model structure of the putative peptide channel. *FEBS Lett 354*:45-49.

Mayer A, Neupert W, Lill R. 1995. Mitochondrial protein import: Reversible binding of the presequence at the *trans* side of the outer membrane drives partial translocation and unfolding. *Cell 80*:127-137.

Merritt EA, Sarfaty S, van den Akker F, L'Hoir C, Martial JA, Hol WGJ. 1994. Crystal structure of cholera toxin B-pentamer bound to receptor $G_{M1}$ pentasaccharide. *Protein Sci 3*:166-175.

Montal M. 1995. Design of molecular function: Channels of communication. *Annu Rev Biophys Biomol Struct 24*:31-57.

Montal M, Anholt R, Labarca P. 1986. The reconstituted acetylcholine receptor. In: Miller C, ed. *Ion channel reconstitution*. New York: Plenum Press. pp 157-204.

Montal MS, Blewitt R, Tomich JM, Montal M. 1992. Identification of the ion channel-forming motif in the primary structure of tetanus and botulinum neurotoxins. *FEBS Lett 313*:12-18.

Montal M, Montal MS, Tomich JM. 1990. Synporins—Synthetic proteins that emulate the pore structure of biological ionic channels. *Proc Natl Acad Sci USA 87*:6929-6933.

Montal M, Mueller P. 1972. Formation of bimolecular membranes from lipid monolayers and a study of their electrical properties. *Proc Natl Acad Sci USA 69*:3562-3566.

Montecucco C, Papini E, Schiavo G. 1991. In: Alouf JE, Freer JH, eds. *A source-book of bacterial protein toxins*. London: Academic Press. pp 45-56.

Montecucco C, Papini E, Schiavo G. 1994. Bacterial protein toxins penetrate cells via a four-step mechanism. *FEBS Lett 346*:92-98

Montecucco C, Schiavo G. 1994. Mechanism of action of tetanus and botulinum neurotoxins. *Mol Microbiol 13*:1-8.

Oblatt-Montal M, Buhler LK, Iwamoto T, Tomich JM, Montal M. 1993. Synthetic peptides and four helix bundle proteins as model systems for the pore-forming structure of channel proteins. I. Transmembrane segment M2 of the nicotinic cholinergic receptor channel is a key pore-lining structure. *J Biol Chem 268*:14601-14607.

Oiki S, Danho W, Madison V, Montal M. 1988. M2δ, a candidate for the structure lining the ionic channel of the nicotinic cholinergic receptor. *Proc Natl Acad Sci USA 85*:8703-8707.

Oiki S, Madison V, Montal M. 1990. Bundles of amphipathic transmembrane α-helices as a structural motif for ion-conducting channel proteins: Studies on sodium channels and acetylcholine receptors. *Proteins Struct Funct Genet 8*:226-236

Rauch G, Gambale F, Montal M. 1990. Tetanus toxin channel in phosphatidylserine planar bilayers: Conductance states and pH dependence. *Eur J Biophys 18*:79-83.

Rothman JE. 1994. Mechanisms of intracellular protein transport. *Nature 372*:55-63.

Schiavo G, Benfenati F, Poulain B, Rosetto O, Polverino de Laureto P, DasGupta BR, Montecucco C. 1992a. Tetanus and botulinum B neurotoxins block neurotransmitter release by proteolytic cleavage of synaptobrevin. *Nature 359*:832-835.

Schiavo G, Rosetto O, Benfenati F, Poulain B, Montecucco C. 1994. Tetanus and botulinum neurotoxins are zinc proteases specific for components of the neuroexocytosis apparatus. *Ann NY Acad Sci 710*:65-75.

Schiavo G, Rosetto O, Catsicas S, Polverino de Laureto P, DasGupta BR, Benfenati F, Montecucco C. 1993a. Identification of the nerve terminal targets of botulinum neurotoxin serotypes A, D, and E. *J Biol Chem 268*:23784-23787.

Schiavo G, Rosetto O, Santucci A, DasGupta BR, Montecucco C. 1992b. Botulinum neurotoxins are zinc proteins. *J Biol Chem 267*:23479-23483.

Schiavo G, Santucci A, Dasgupta BR, Mehta PP, Jontes J, Benfenati F, Wilson MC, Montecucco C. 1993b. Botulinum neurotoxins serotypes A and E cleave SNAP-25 at distinct COOH-terminal peptide bonds. *FEBS Lett 335*:99-103.

Schmid A, Benz R, Just I, Aktories K. 1994. Interaction of *Clostridium botulinum* C2 toxin with lipid bilayer membranes. Formation of cation-selective channels and inhibition of channel function by chloroquine. *J Biol Chem 269*:16706-16711.

Schmid MF, Robinson TP, DasGupta BR. 1993. Direct visualization of bot-

ulinum neurotoxin-induced channels in phospholipid vesicles. *Nature 364*:827–830.

Schnolzer M, Alewood P, Jones A, Alewood D, Kent SB. 1992. In situ neutralization in Boc-chemistry solid phase peptide synthesis. Rapid, high yield assembly of difficult sequences. *Int J Pept Protein Res 40*:180–193.

Simon SM, Blobel G. 1991. A protein-conducting channel in the endoplasmic reticulum. *Cell 65*:371–380.

Simon SM, Blobel G. 1992. Signal peptides open protein-conducting channels in *E. coli*. *Cell 69*:677–684.

Simpson LL, ed. 1989. *Botulinum neurotoxin and tetanus toxin*. San Diego, California: Academic Press. pp 153–178.

Sixma TK, Kalk KH, vanZanten BA, Dauter Z, Kingma J, Witholt B, Hol WG. 1993a. Refined structure of *Escherichia coli* heat-labile enterotoxin, a close relative of cholera toxin. *J Mol Biol 230*:890–918.

Sixma TK, Stein PE, Hol WG, Read RJ. 1993b. Comparison of the B-pentamers of heat labile enterotoxin and verotoxin-1: Two structures with remarkable similarity and dissimilarity. *Biochemistry 32*:191–198.

Smart OS, Goodfellow JM, Wallace BA. 1993. The pore dimensions of gramicidin A. *Biophys J 65*:2455–2460.

Sollner T, Rothman JE. 1994. Neurotransmission: Harnessing fusion machinery at the synapse. *Trends Neurosci 173*:44–48.

Stein PE, Boodhoo A, Tyrrell GJ, Brunton JL, Read RJ. 1992. Crystal structure of the cell binding B oligomer of verotoxin-1 from *E. coli*. *Nature 355*:748–750.

Stevens RC, Evenson ML, Tepp W, DasGupta BR. 1991. Crystallization and preliminary X-ray analysis of botulinum neurotoxin A. *J Mol Biol 222*: 877–880.

Suarez-Isla BA, Wan K, Lindstrom J, Montal M. 1983. Single-channel recordings from purified acetylcholine receptors reconstituted in bilayers formed at the tip of patch pipets. *Biochemistry 22*:2319–2323.

Unwin N. 1993. Nicotinic acetylcholine receptor at 9 Å resolution. *J Mol Biol 229*:1101–1124.

Unwin N. 1995. Acetylcholine receptor channel imaged in the open state. *Nature 373*:37–43.

Yamasaki S, Baumeister A, Binz T, Blasi J, Link E, Cornille F, Roques B, Fykse EM, Sudhof TC, Jahn R, Niemann H. 1994. Cleavage of members of the synaptobrevin/VAMP family by types D and F botulinal neurotoxins and tetanus toxin. *J Biol Chem 269*:12764–12772.